Scheme VI. Mechanism of Inhibition of Thermolysin by HONH-Ibm-Ala-GlyNH$_2$

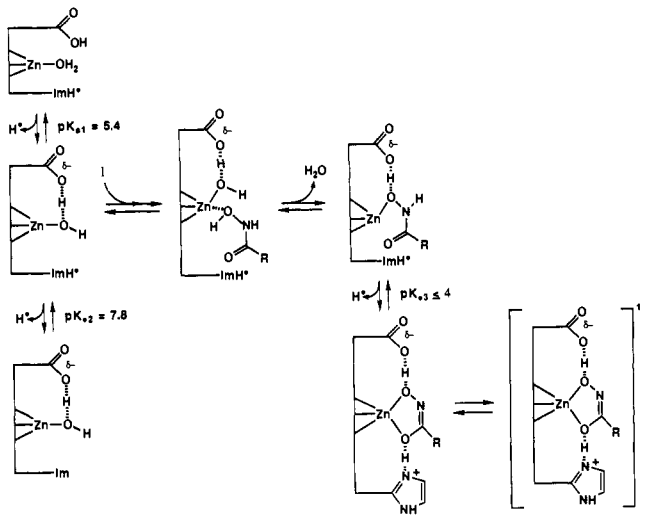

to an encounter complex in which both inhibitor and zinc-bound water are present in the active site.

Summary: Mechanism of Inhibition of Thermolysin by HONH-Ibm-Ala-GlyNH$_2$. The mechanism that we propose for the inhibition of thermolysin by the hydroxamic acid HONH-Ibm-Ala-GlyNH$_2$ is shown in Scheme VI. Essential features of this mechanism are as follows: (1) For productive complex formation with the inhibitor, thermolysin must be in the same ionization state that is required for catalysis. While we cannot rule out interaction of inhibitor with other ionized states of thermolysin, the initial complexes that result from these interactions will not be productive and go on to form stable complexes. Furthermore, it is the neutral, un-ionized form of the hydroxamic acid that binds to TLN, not the hydroxamate anion as suggested previously.[4-6] (2) Formation of the initial monodentate complex with displacement of the zinc-bound water molecule is a two-step process. This is required to avoid the energetically unfavorable mechanism involving dissociation of H_2O–ZnL_3 to ZnL_3 followed by complexation of inhibitor with ZnL_3. Thus, in the multistep reaction that we propose in Scheme VI, transfer of the zinc-bound water to bulk solvent occurs early on the pathway, prior to formation of stable complexes. (3) Formation of the stable bidentate complex is accompanied by ionization of the bound hydroxamic acid. This ionization is both necessary, since it is the anion of hydroxamic acids that interacts strongly with metal ions, and allowed, since at neutral pH the pK_a of the hydroxamic acid, like H_2O, will have been lowered upon interaction with the zinc. (4) At elevated temperatures, another complex accumulates. It is unclear what the structure of this complex is, but it may be a conformational isomer of the bidentate complex that is stable and accumulates at lower temperatures.

Acknowledgment. Thanks goes to Richard K. Harrison (Enzymology Department, Merck) for determining the pK_a of HONH-Ibm-Ala-GlyNH$_2$.

Characterization of the Structural Properties of α_1B, a Peptide Designed To Form a Four-Helix Bundle

John J. Osterhout, Jr.,[†] Tracy Handel,[‡] George Na,[§] Arazdordi Toumadje,[∥] Robert C. Long,[⊥] Peter J. Connolly,[†] Jeffrey C. Hoch,[†] W. Curtis Johnson, Jr.,[∥] David Live,*[,⊥] and William F. DeGrado*[,‡]

Contribution from the Central Research and Development Department, E. I. duPont de Nemours and Company, Experimental Station, Building 328, Wilmington, Delaware 1988-3028, The Rowland Institute for Science, 100 Cambridge Parkway, Cambridge, Massachusetts 02142, Sterling Research Group, 25 Great Valley Parkway, Malvern, Pennsylvania 19355, Department of Biochemistry and Biophysics, Oregon State University, Corvallis, Oregon 97331, and Department of Chemistry, Emory University, 1515 Pirece Drive, Atlanta, Georgia 30322.
Received March 8, 1991

Abstract: The structural and dynamic properties of α_1B, a peptide designed to self-associate into a four-helix bundle protein, have been examined using sedimentation equilibrium centrifugation, vacuum UV CD spectroscopy, and NMR spectroscopy. The peptide cooperatively forms tetramers, and the stability of the tetramer depends markedly on pH. CD and NMR spectroscopy indicate that the central core of the peptide is fully α-helical, and the N-terminal and C-terminal residues are structurally less well-defined. The NMR spectra are consistent with the symmetry of the designed tetramer and also suggest that the individual peptides in the tetramer dissociate to form monomers at rates that are intermediate to slow on the NMR time scale.

The mechanism by which proteins fold into their native, well-defined structures is a major, unsolved problem. One approach to the study of this problem involves the de novo design of proteins.[1-12] A rational strategy involves the design of sequences expected to display one of the basic motifs of protein structure (e.g., helix or sheet) and the evaluation of the correlation between the predicted and observed structural properties of these designs. Such sequences can then be elaborated into peptides and proteins that adopt supersecondary and tertiary structures with predictable structures and functions. Feedback from structural and functional studies plays an important role for iteratively improving the designs.

[†] The Rowland Institute.
[‡] DuPont.
[§] Sterling Research Group.
[∥] Oregon State University.
[⊥] Emory University.

(1) (a) DeGrado, W. F. *Adv. Protein Chem.* **1988**, *39*, 51-124. (b) DeGrado, W. F.; Wasserman, Z. R.; Lear, J. D. *Science* **1988**, *243*, 622-628.
(2) Gutte, B.; Däumigen, M.; Wittschieber, E. *Nature (London)* **1979**, *281*, 650-655.

0002-7863/92/1514-331$03.00/0

The four-helix bundle[13] is one basic structural element that has attracted significant attention in protein engineering[1,3,5-12] and, in particular, has served as an early target for the minimalist approach to protein design.[1] In an iterative strategy aimed at the design of proteins with this motif (Figure 1), several α-helical peptides were designed that were subsequently shown to assemble into tetramers.[8,9] The peptides contained leucine residues along one face of the helix, intended to stabilize tetramerization through hydrophobic forces, while the hydrophilic face contained glutamate and lysine residues, intended to electrostatically stabilize helix formation. The free energies of tetramerization of these peptides were assessed by monitoring the concentration dependence of their CD spectra. The most favorable free energy of association (−22 kcal/mol) was exhibited by the peptide α_1B (Figure 1). The next step of the incremental design process was to incorporate a loop sequence between two copies of α_1B.[8,9] This peptide, α_2, was shown to dimerize as measured by the concentration dependence of the CD spectra.[9] The final step was to connect two dimers with loop sequence to produce a complete four-helix bundle protein, α4. This was accomplished by gene synthesis, and the protein was expressed in bacteria.[10,11] The structural and thermodynamic properties of α_1B, α_2, and α_4 have been characterized by CD spectroscopy and size exclusion chromatography, which indicated that they adopt stable helical structures in aqueous solution.[8-11]

Detailed structural studies of these systems are now being undertaken by NMR spectroscopy and X-ray crystallography. Eisenberg and co-workers have recently determined the crystal structure of a 12-residue α_1 peptide.[14] This peptide is related to α_1B and appears to form tetramers at neutral physiological salt concentrations as judged from CD spectra although the association was weaker than that exhibited by α_1B (the midpoint for tetramerization is in excess of 1 mM as compared to <10 μM for α_1B). The crystal structure shows some of the design features—the peptide is α-helical from residues one to nine, with the leucine side chains forming hydrophobic associations with another monomer unit to form an antiparallel dimer. Three dimers hydrophobically associate to form a hexamer. Dimers of neighboring hexamers abut forming tetramers, although the interhelical crossing angle is wider than that typically observed in four-helix bundles. In contrast, Feigon and co-workers have examined this α_1 peptide in solution by NMR and find evidence for helical structure throughout its entire length.[15] The reasons for the discrepancy between the CD data and the X-ray data might be related to the relatively low stability of the tetrameric form of this peptide and the effects of crystal packing forces.

In the current manuscript we describe the characterization of the structural properties of the 16-residue peptide, α_1B, in aqueous solution by equilibrium sedimentation centrifugation, two-dimensional NMR spectroscopy, and vacuum UV CD spectroscopy.

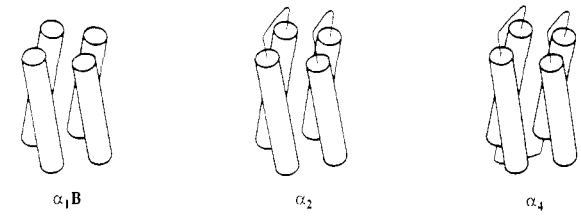

Helix = GlyGluLeuGluGluLeuLeuLysLysLeuLysGluLeuLeuLysGly

Loop = ProArgArg

α_1B = Ac-Helix-$CONH_2$

α_2 = Ac-Helix-Loop-Helix-$CONH_2$

α_4 = Met-Helix-Loop-Helix-Loop-Helix-Loop-Helix-COOH

Figure 1. Schematic representation of the desired conformations of α-helical peptides and their amino acid sequences.

Experimental Section

Materials and Methods. Peptides and proteins were synthesized and purified as described previously.[9,11]

NMR Studies. Samples for NMR studies were prepared in 90% ^1H_2O/10% ^2H_2O, 0.02 M NaCl with 20 μM TSP, 3-(trimethylsilyl)-propionic-*2,2,3,3-*$^2H_4$ acid sodium salt, added as a chemical shift reference. The pH was adjusted to 3.0 or 5.0 with dilute NaOH and HCl solutions. pH readings were uncorrected for isotope effects. The peptide concentration was determined by integration of selected peptide resonances and comparison to internal TSP or by amino acid analysis.

Two-dimensional NMR spectra were obtained on JEOL JNM-GX400, Bruker AM-600, and GE GN-600 spectrometers. For assignment purposes COSY,[16] NOESY,[17] and clean TOCSY[18] experiments were performed in the phase-sensitive mode according to the method of States et al.[19] The water resonance was suppressed by gated irradiation during the delay times (2 s) and during the mixing time in the NOESY experiments. Mixing times for the NOESY experiments were either 50 or 200 ms as indicated. TOCSY experiments were performed with mixing times of 60–80 ms. The data were processed with Lorentz to Gaussian transformation or phase shifted sine bell apodization and zero filled to produce spectra with 2048 complex points in each dimension. The spectral width was 4307 Hz and the carrier frequency was centered on the water peak. Data were processed with software developed at the Rowland Institute for Science[20] using either a VAX 8250 or an Ardent Titan computer. All spectra were processed for t_1 ridge suppression[21] and baseline correction before the ω_1 transform.[22] Spectral conditions at 600 mHz were similar, and data were processed with either FT-NMR (Hare Research) or software provided by GE. 1-D spectra were also obtained at 600 MHz in 90% H_2O/10% ^2H_2O. The latter were taken as the first slice of a NOESY experiment using a 5 ms mixing time and 1.5 s relaxation delay during which the water resonance was irradiated.

pH-Dependent CD Studies. The dependence of the ellipticity at 222 nm (θ_{222}) on peptide concentration was determined and analyzed as described previously.[9] In these studies, samples were prepared in a ^2H_2O solution (to allow comparison with hydrogen–deuterium exchange studies) containing 3.0 mM each of sodium borate, sodium phosphate, and sodium citrate adjusted to pH as indicated (uncorrected for isotope effects).

Vacuum UV CD Spectroscopy. CD spectra were measured at 20 °C over the range 260–178 nm using a vacuum ultraviolet spectrometer.[23] Spectra were scanned at 1 nm per minute and digitized at half nanometer intervals. The peptide or protein concentration was approximately 1 mg/mL in 0.01 M 3-(*N*-morpholino)propanesulfonic acid (MOPS)

(3) (a) Richardson, J. S.; Richardson, D. C. *Protein Engineering*; Alan R. Liss: New York, **1987**; pp 149–163. (b) Hecht, M. H.; Richardson, J. S.; Richardson, D. C.; Ogden, R. C. *Science* **1990**, *249*, 884–892.
(4) (a) Hodges, R. S.; Zhou, N. E.; Kay, C. M.; Semchuk, P. D. *Peptide Res.* **1990**, *3*, 123–137. (b) Lau, S. Y. M.; Taneja, A. K.; Hodges, R. S. *J. Biol. Chem.* **1984**, *259*, 13253–13261.
(5) (a) Mutter, M.; Vuilleumier, S. *Angew. Chem. Int. Ed.* **1989**, *28*, 535–554. (b) Ernest, I.; Vuilleumier, S.; Fritz, H.; Mutter, M. *Tetrahedron Lett.* **1990**, *31*, 4015–4018.
(6) Sasaki, T.; Kaiser, E. T. *J. Am. Chem. Soc.* **1989**, *111*, 380–381.
(7) Hahn, K. W.; Klis, W. A.; Stewart, J. M. *Science* **1990**, *248*, 1544–1547.
(8) Eisenberg, D.; Wilcox, W.; Eshita, S. M.; Pryciak, P. M.; Ho, S. P.; DeGrado, W. F. *Proteins* **1986**, *1*, 16–22.
(9) Ho, S. P.; DeGrado, W. F. *J. Am. Chem. Soc.* **1987**, *109*, 6751–6758.
(10) DeGrado, W. F.; Regan, L.; Ho, S. P. *Cold Spring Harbor Symp. Quant. Biol.* **1987**, *L11*, 521–526.
(11) Regan, L.; DeGrado, W. F. *Science* **1988**, *241*, 976–979.
(12) Handel, T.; DeGrado, W. F. *J. Am. Chem. Soc.* **1990**, *112*, 6710–6711.
(13) Weber, P. C.; Salemme, F. R. *Nature (London)* **1980**, *287*, 82–84.
(14) Hill, C. P.; Anderson, D. H.; Wesson, L.; DeGrado, W. F.; Eisenberg, D. *Science* **1990**, *249*, 543–546.
(15) Ciesla, D. S.; Gilbert, D. E.; Feigon, J. *J. Am. Chem. Soc.* **1991**, *113*, 3957–3961.
(16) Marion, D.; Wüthrich, K. *Biochem. Biophys. Res. Commun.* **1983**, *113*, 967–874.
(17) Jeener, J.; Meier, B. H.; Bachmann, P.; Ernst, R. R. *J. Chem. Phys.* **1979**, *71*, 4546–4553.
(18) Griesinger, C.; Otting, G.; Wüthrich, K.; Ernst, R. R. *J. Am. Chem. Soc.* **1988**, *110*, 7870–7872.
(19) States, D. J.; Haberkorn, R. A.; Ruben, D. J. *J. Magn. Reson.* **1982**, *48*, 286–292.
(20) Hoch, J. C. *Rowland Institute for Science Technical Memo*; 1985, No. 18t.
(21) Otting, G.; Senn, H.; Wagner, G.; Wüthrich, K. *J. Magn. Reson.* **1986**, *70*, 500–505.
(22) Zuiderweg, E. R. P.; Boelens, R.; Kaptein, R. *Biopolymers* **1985**, *24*, 601–611.
(23) Johnson, W. C., Jr. *Rev. Sci. Instrum.* **1971**, *42*, 1283–1286.

buffer, pH 7.0, for measurement in a 0.005 cm path length cell. To reduce absorption artifacts in the CD measurements, the total optical densities of the solutions were less than 1.0 at all wavelengths. The instrument was calibrated with (+)-10-camphorsulfonic acid assuming $\Delta\epsilon$ of 2.36 at 290.5 nm and −4.9 at 192.5 nm (the relationship between $\Delta\epsilon$ and the molar ellipticity (θ) in deg cm^2 dmol^{-1} is $[\theta] = 3300\ \Delta\epsilon$).

Analysis of UV CD Spectra. The spectra were analyzed using the method of Hennessey and Johnson,[24] modified to use a statistical method called "variable selection".[25,26] It is necessary to measure the CD spectra of proteins to at least 184 nm if these spectra are to have the information content for reliable prediction of secondary structure.[24] All proteins were analyzed for secondary structures: helix (H), antiparallel β-sheet (A), parallel β-sheet (P), β-turns (T), and the other structures not included in the preceding categories (O). The goal of the analysis is to describe the secondary structural content of a protein or peptide in terms of fractions of each of these secondary structures. The spectrum of a protein depends not only on these five structural groups but also on aromatic side chains, prosthetic groups, twists in the strands of β-sheets, etc. Variable selection helps overcome the problem that the analysis is still underdetermined by removing proteins from the basis set whose CD spectra contain factors not present in the protein being analyzed. Since we do not know in advance which proteins should be eliminated from the basis set, calculations are performed for all possible combinations. Satisfactory combinations must meet the following criteria: (1) the total of the coefficients for all five structures should add up to 1.0 ± 0.05; (2) negative coefficients associated with a given secondary structure should decrease in magnitude as proteins are removed from the basis set, and ultimately should not exceed −0.05; (3) the average root-mean-square error should be consistent with the noise level of the data, about 0.25 $\Delta\epsilon$ units; and (4) the combinations meeting the above criteria and also having the largest number of proteins should be averaged to give the final results. In this work 5 proteins were removed from the original 22 to give combinations that met the above criteria. Concentrations were determined by amino acid analysis. This in turn allowed us to determine the intensity of the 190 nm absorption bands: $\epsilon = 6200\ M^{-1}\ cm^{-1}$ for the α_1B and α_2 peptides and 7500 $M^{-1}\ cm^{-1}$ for the α_4 proteins (values given per residue in each case).

Equilibrium Sedimentation. Equilibrium sedimentation was performed with a Beckman Model E analytical ultracentrifuge. The cell was assembled from a six-channel centerpiece and sapphire windows and loaded with three samples of α_1B with concentrations in the range of 0.1–0.4 mg/mL. A buffer containing 0.01 M sodium phosphate and 0.1 M NaCl at pH 7.0 was used. The centrifugation proceeded at 20 °C and 36 000 rpm for 30 h. The distribution of α_1B within the cell was determined by measuring the absorbance with an optical scanner at 232 nm. Scans were also collected at 260 nm where α_1B does not absorb appreciably to be used as the baseline. The slit of the photomultiplier was set at 0.1 mm and the slit of the monochromator was at 2 mm. The scan rate was 0.0542 mm/s. The analog signal of the scanner was sent to a microcomputer where it was converted to digital form by a 12-bit analog-to-digital converter. The analog signal was sampled every 10 ms and the average of every 25 readings was recorded on a diskette as a data point. Each recorded scan consisted of 1200 data points. Fifteen scans were collected and averaged to give the final best-smoothed data. For the purpose of calibration, scans were also collected immediately after the rotor had reached the top speed to determine the initial absorbance, in voltage unit, of the samples. The initial absorbance was then plotted against the loading peptide concentration to ascertain the linearity of the scanner data and obtain the extinction coefficient of the peptide in units of V mL mg^{-1}. The latter number was used to convert the equilibrium scan from voltage to concentration unit. A partial specific volume of 0.788 mL/g for α_1B was calculated from the partial specific volumes of the constituent amino acids[28] and used in deriving the apparent average molecular weight. The density of the buffer was determined with an Anton-Parr Model DMA-02 precision density meter.

Results and Discussion

Sedimentation Equilibrium Centrifugation. Figure 2 shows the apparent average molecular weight of α_1B as a function of concentration. From 0.06 to 0.2 mg/mL, the average molecular weight increased with increasing concentration. At concentrations above that range, the average molecular weight leveled off and approached asymptotically that of the tetramer. The data, therefore, indicate a strong self-association of α_1B into tetramers, and the lack of higher order aggregates. Theoretical curves were calculated according to a model of cooperative monomer–tetramer self-association

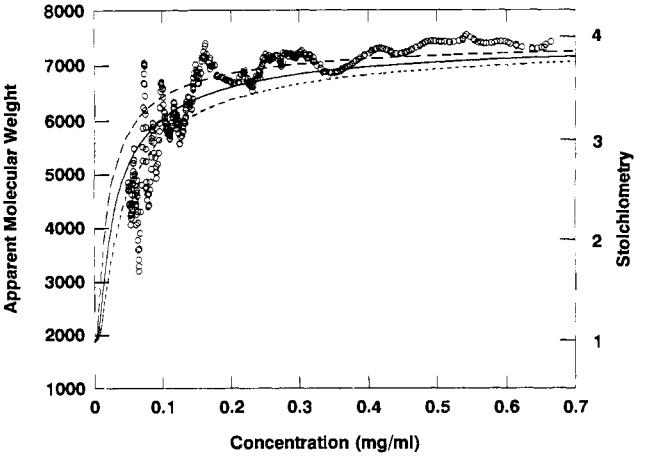

Figure 2. Apparent average molecular weight of α_1B derived from equilibrium sedimentation and plotted against the concentration of the peptide. The solid curve represents the best fit of the data by the monomer–tetramer association model described by eq 1 using a monomer molecular weight of 1880 and $K = 2.5 \times 10^{14}\ M^{-3}$. Also shown are two additional theoretical curves (long and short dashed lines) calculated by using $K = 10^{15}$ and $10^{14}\ M^{-3}$, respectively.

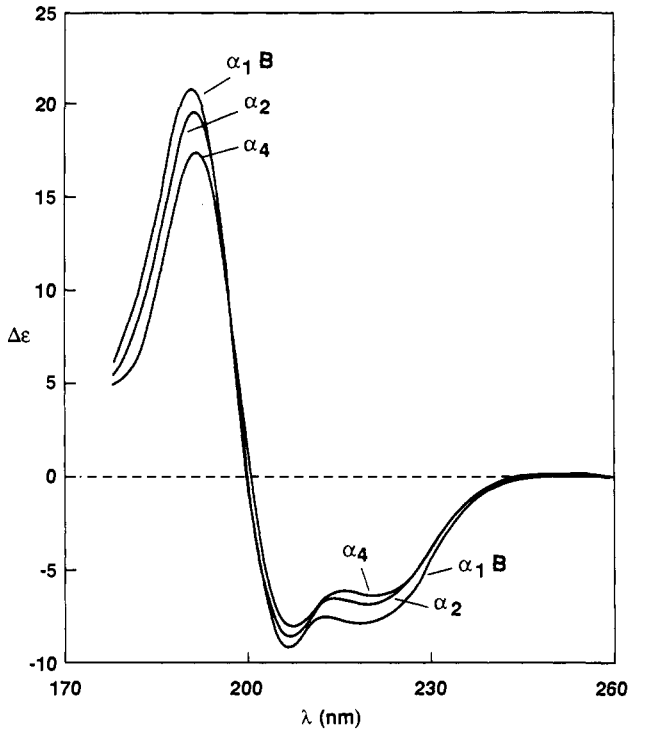

Figure 3. Vacuum UV CD spectrum of α_1B, α_2, and α_4.

Scheme I

$$4M \overset{K_{ass}}{\rightleftharpoons} T$$

where M and T refer to the monomer and tetramer, respectively, and the self-association constant, K_{ass}, can be expressed as

$$K_{ass} = [T]/[M]^4 \qquad (1)$$

The solid curve in Figure 2 represents the least-squares fitting of the data which has an association constant on the order of

(24) Hennessey, J. P.; Johnson, W. C., Jr. *Biochemistry* **1981**, *20*, 1085–1094.
(25) (a) Manavalan, P.; Johnson, W. C., Jr. *Anal. Biochem.* **1987**, *167*, 76–85. (b) Mosteller, F.; Tukey, J. W. *Data Analysis and Regression*; Addison-Wesley: Reading, MA, 1977.
(26) Johnson, W. C. *Proteins* **1990**, *7*, 205–214.
(27) Manavalan, P.; Johnson, W. C., Jr. *Nature (London)* **1983**, *305*, 831–832.

Table I. Estimates of the Secondary Structural Content of α-Helical Peptides Based on CD Analysis[a]

	H	A	P	T	O	total
α_1B	0.78 (0.01)	0.02 (0.01)	0.01 (0.01)	0.22 (0.02)	0.01 (0.01)	1.04
α_2	0.74 (0.02)	0.1 (0.01)	0.00	0.25 (0.01)	0.01 (0.02)	1.00
α_4	0.73 (0.03)	0.04 (0.03)	0.01 (0.01)	0.24 (0.02)	0.01 (0.01)	1.03

[a] Conditions and definitions of symbols are given in the Experimental Section. The standard deviation of the analyses is given in parentheses.

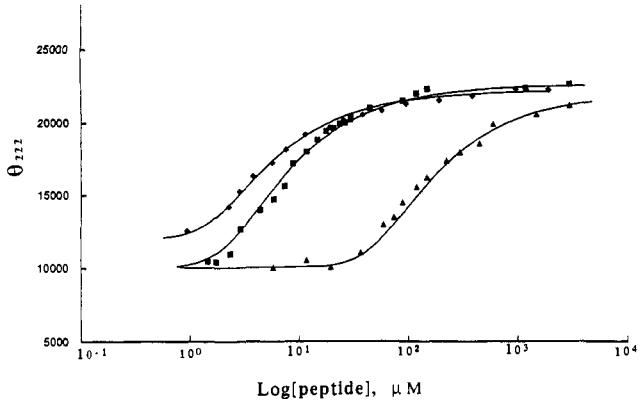

Figure 4. The dependence of θ_{222} on peptide concentration at pH 3.0 (▲), 5.0 (■), and 7.0 (♦) under conditions described in the Experimental Section. The data were fit by theoretical curves describing monomer–tetramer equilibria as described previously.[9] Parameters used to generate the curves are summarized in Table II.

Table II. Summary of the Free Energy of Tetramerization (ΔG), the Tetramer Ellipticity (Maximum Negative Intensity at θ_{222}), and the Monomer Ellipticity (Minimum Negative Intensity θ_{222}) at pH 3.0, 5.0, and 7.0[a]

		θ_{222} (deg cm^2 dmol^{-1})	
pH[b]	ΔG (kcal/mol)	max	min
3.0	−16.0	22000	10000
5.0	−18.8	22500	10000
7.0	−20.6	22200	12000

[a] Values were determined by fitting the data in Figure 4 to expressions for monomer–tetramer equilibria as previously described.[9] [b] Uncorrected for isotope effects.

between 10^{14} and 10^{15} M^{-3}, in reasonable agreement with that described by examination of the concentration dependence of the CD spectrum (8.1×10^{14} M^{-3}, see within). It should be pointed out that the association constant derived from equilibrium sedimentation has a greater degree of uncertainty due to the scattering of the data at low peptide concentrations.

Vacuum UV CD. The CD spectrum of α_1B in the tetrameric state exhibits minima at approximately 207 and 222 nm, and a maximum at 191 nm (Figure 3). This distinctive shape and the fact that the short wavelength crossover will be below 175 nm is characteristic of all α-helical proteins.[28] Analysis of the CD spectra for secondary structure (Table I) predicts negligible amounts of antiparallel β-sheet, parallel β-sheet, and "other" structure. With its acetyl and carboxamide end groups, α_1B has 17 chromophoric amide groups, 13 of which are predicted to be in an α-helix. The remaining four amide groups are predicted to occur in turns, which could include type III turns or 3_{10} helix. It is interesting to note that the C-terminus of α-helices in the crystal structures of peptides and proteins is often terminated by one or more residues of 3_{10} helix.[29]

For comparison, the spectra of α_2 and α_4 are also illustrated in Figure 3. Analysis of their secondary structure (Table I) predicts that the α_2 contains 27 amide groups in an α-helical conformation, and α_4 contains 53 α-helical residues. Thus, within experimental error, the number of amide groups in an α-helical conformation is predicted to be the same for the α_1B tetramer

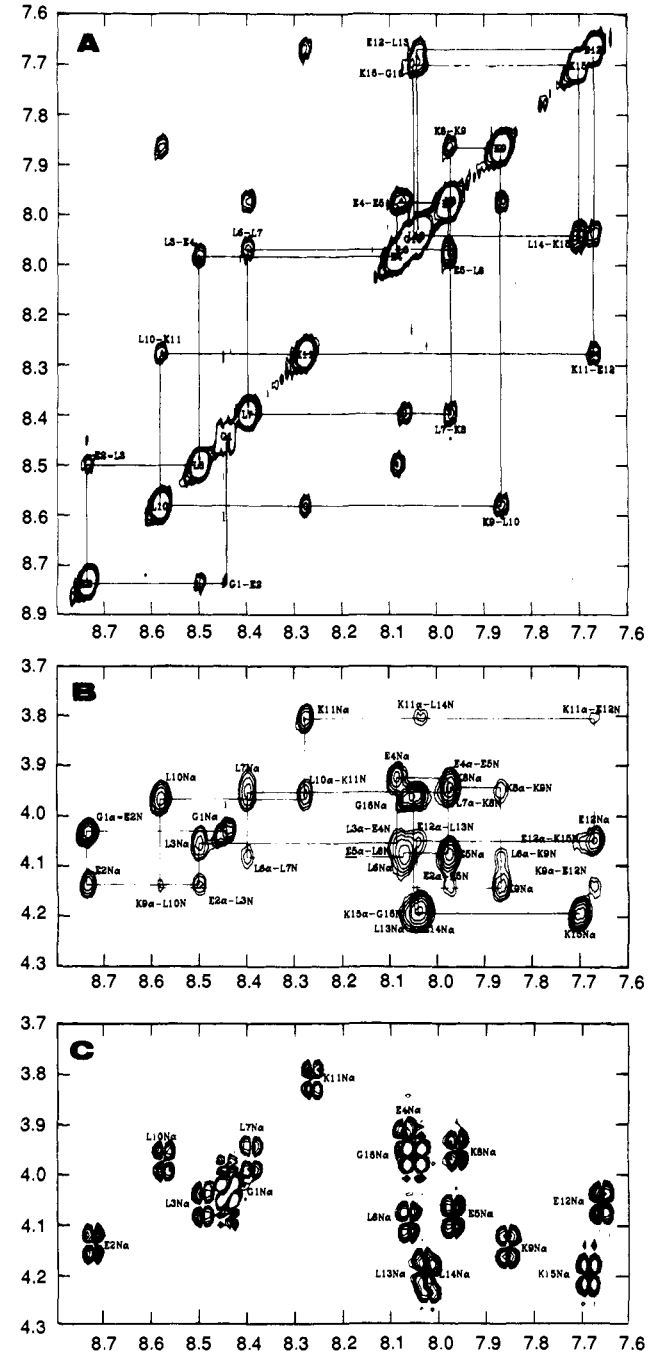

Figure 5. Two-dimensional NMR spectra of α_1B at pH 5.0: a portion of the NOESY spectrum showing (A) the amide resonances and the amide–amide cross peaks, and (B) the crosspeaks between amide and C_α protons. A portion of the COSY spectrum showing the crosspeaks between amide and C_α protons is shown in C. Spectra were acquired on a JEOL JNM-GX400 spectrometer in the phase sensitive mode according to the method of States et al.[19] 256 slices were acquired with 2048 data points. The data were apodized with Lorentz to Gaussian transformation in t_2 and a 60° phase shifted sine bell in t_1. The spectra were zero filled to yield a 2048 by 2048 square matrix.

(4 × 13 = 52 amide groups), the α_2 dimer (2 × 27 = 54 amide groups), and the α_4 protein (53 amide groups). This finding

(28) Cohn, E. J.; Edsall, J. T. *Proteins, Amino Acids and Peptides as Ions and Dipolar Ions*; Reinhold, New York, 1943; pp 370–381.
(29) Richardson, J. *Adv. Protein Chem.* **1981**, *34*, 167–339.

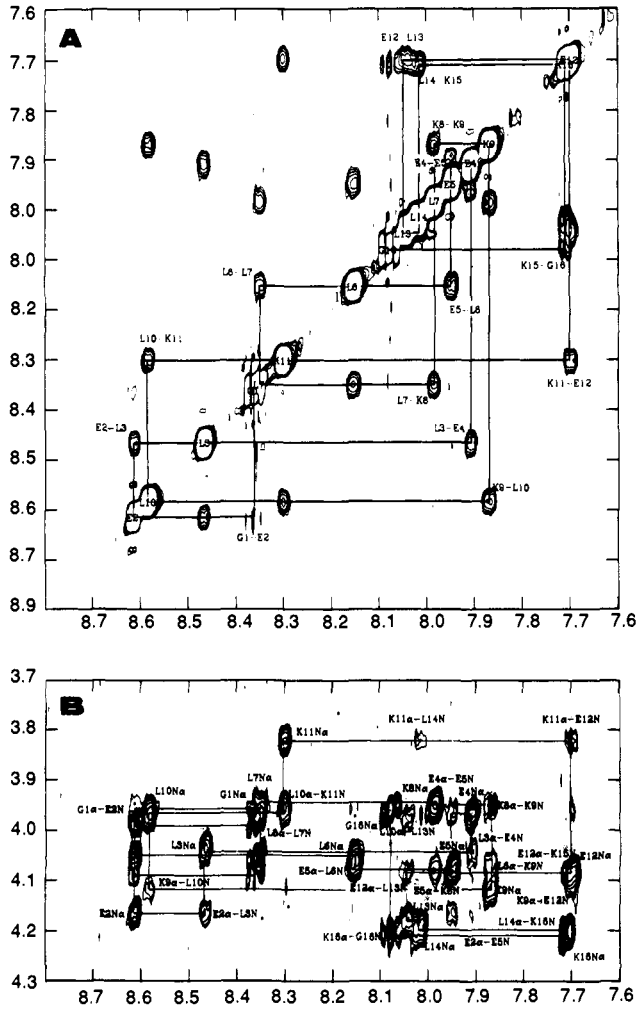

Figure 6. Portions of a NOESY spectrum of α_1B at pH 3.0 showing (A) the amide resonances and amide–amide crosspeaks and (B) amide to C_α proton crosspeaks. The data were processed as in Figure 5 except they were processed to a 1024 by 1024 matrix.

supports the guiding hypothesis that the unlinked and linked helices will assemble into similar structures and suggests that the structural results reported here for α_1B may be relevant to the structure of the full length α_4 protein.

pH Dependence of the Association of α_1B. NMR spectroscopy of peptides in water is most easily accomplished in the mildly acidic pH range, where exchange of amide protons with solvent is relatively slow.[30] Therefore, to determine whether α_1B also formed tetramers at low pH, we examined its self-association at pH 3.0, 5.0, and 7.0 using circular dichroism (Figure 4). This was accomplished as described previously[6,8] by analyzing the ellipticity at 222 nm (θ_{222}, a measure of the α-helical content) as a function of peptide concentration. In each case θ_{222} shows a fourth order dependence on peptide concentration, consistent with the formation of a tetramer. Also, the limiting value of θ_{222} extrapolated to infinite peptide concentration was independent of pH, suggesting that an aggregate with the same degree of secondary structure was formed between pH 3.0 and 7.0. In contrast, the free energies of association became less favorable as the pH was lowered, and a concomitant decrease in the helical content of the monomeric form of the peptide was also observed (Table II). These data suggest that lowering the pH in the acid range alters the stability of the tetramer, presumably through protonation of Glu residues, but does not substantially alter the secondary structural content of the tetramer.

(30) (a) Molday, R. S.; Englander, S. W.; Kallen, R. G. *Biochemistry* **1972**, *11*, 150–158. (b) Englander, W. S.; Kallenbach, N. R. *Q. Rev. Biophys.* **1984**, *16*, 521.

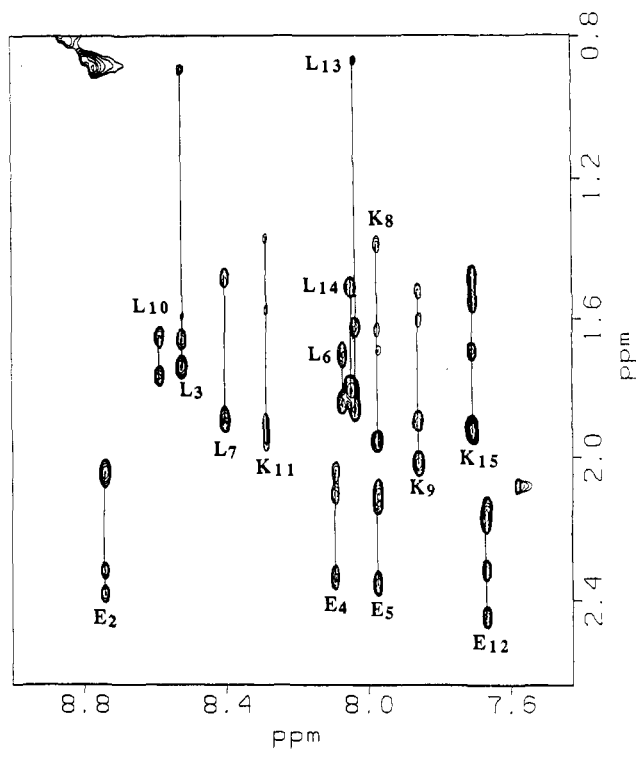

Figure 7. Amide to aliphatic region of a 66-ms TOCSY experiment of α_1B at pH 5.0, 22 °C. The spectra were acquired on a Bruker AM-600 in pure-phase absorption mode using the time-proportional incrementation method[38] with 512 increments of 2K data points. Both dimensions were apodized with a 60° phase-shifted sine bell.

The aggregation state of α_1B was also examined by size exclusion chromatography. The peptide had previously been shown to elute at the volume expected for a tetramer at pH 7.0.[9] It eluted at an identical volume at pH 5.0, indicating that a tetramer is also formed at pH 5.0. The association at pH 3.0 was too weak to be analyzed by this method.

NMR Studies. Sequence specific assignments were obtained much as described by Wüthrich.[31] COSY and TOCSY experiments were used to establish amino acid spin systems, and NOESY experiments were used to provide sequential connectivities.

Figure 5 illustrates selected regions of the NOESY and COSY spectra of α_1B at pH 5.0 and 25 °C. Sequential $d_{\alpha N}(i,i+1)$ NOEs are observed in the NOESY spectrum from Gly 1 to Leu 3 and from Leu 6 to Leu 13 (Figure 5). The assignment of Gly 1 is determined by a cross peak between the Gly 1 amide proton and the acetyl methyl group (not shown). Sequential $d_{NN}(i,i+1)$ NOEs from Leu 3 to Leu 6 establish the connectivity of the peptide backbone. The amide to α cross peaks of Leu 13 and Leu 14 are overlapped preventing the observation of either $d_{\alpha N}(i,i+1)$ or $d_{NN}(i,i+1)$ NOEs between them. A $d_{NN}(i,i+1)$ NOE between Leu 14 and Lys 15 locates the amide proton resonance of Leu 14. A $d_{\alpha N}(i,i+1)$ NOE is observed between Lys 15 and Gly 16. The assignment of Gly 16 was also confirmed by the observation of cross peaks between the Gly 16 α proton and the terminal carboxamide protons. The assignments of the side chain resonances were determined largely from the amide to side chain and α to side chain regions of clean TOCSY spectra (the amide to side chain portion of a TOCSY spectrum of α_1B is presented in Figure 7).

The assignment of α_1B at pH 3.0 was achieved in a similar manner. Portions of the NOESY spectrum of α_1B at pH 3.0, 25 °C, are presented in Figure 6. The complete resonance assignments of α_1B at pH 5.0 and 3.0 are presented in Tables III and IV.

The NOEs observed in α_1B at pH 5.0 are summarized in Figure 8. Stretches of $d_{NN}(i,i+1)$ NOEs along with $d_{\alpha N}(i,i+3)$ and $d_{\alpha\beta}(i,i+3)$ NOEs are characteristic of α-helices.[31] In α_1B at pH 5.0 fourteen of the fifteen possible $d_{NN}(i,i+1)$ NOEs are observed

Table III. NMR Assignments for α_1B at pH 5.0

residue	NH	α	β	γ	δ	ε
Gly 1	8.44	4.03				
Glu 2	8.73	4.13	2.06, 2.03	2.34, 2.40		
Leu 3	8.49	4.06	1.66, 1.74	1.59	0.91	
Glu 4	8.07	3.90	2.08, 2.12	2.34, 2.37		
Glu 5	7.97	4.08	1.98, 2.13	2.32, 2.35		
Leu 6	8.06	4.09	1.87	1.75	0.86, 0.98	
Leu 7	8.39	3.97	1.91, 1.90	1.53	0.82	
Lys 8	7.96	3.94	1.98	1.41	1.71, 1.63	2.97
Lys 9	7.86	4.13	2.06, 1.92	1.55, 1.63	1.70	2.98
Leu 10	8.58	3.97	1.79	1.67	0.80, 0.76	
Lys 11	8.26	3.81	1.96, 1.92	1.40, 1.60	1.69	2.92
Glu 12	7.67	4.05	2.17, 2.18	2.46, 2.34		
Leu 13	8.03	4.19	1.85	1.64	0.89	
Leu 14	8.03	4.22	1.83	1.53	0.84	
Lys 15	7.69	4.20	1.94	1.54	1.73	3.01
Gly 16	8.05	3.96				
acetyl methyl	2.10					
$-NH_2$	7.43, 7.18					

Table IV. NMR Assignments for α_1B at pH 3.0

residue	NH	α	β	γ	δ	ε
Gly 1	8.34	4.11				
Glu 2	8.625	4.23	2.19, 2.12	2.56, 2.52		
Leu 3	8.454	4.10	1.78	1.67		
Glu 4	7.93	4.02	2.17	2.56		
Glu 5	7.96	4.13	2.25, 2.20	2.57		
Leu 6	8.17	4.12	1.92, 1.82	1.72	0.94, 0.91	
Leu 7	8.37	4.02	1.93	1.57	0.94	
Lys 8	8.01	3.99	1.99, 1.86	1.45	1.75, 1.68	3.03
Lys 9	7.89	4.17	2.06, 1.95	1.57	1.75, 1.66	3.03
Leu 10	8.61	4.03	1.85	1.70	0.93	
Lys 11	8.33	3.89	1.99	1.45	1.74, 1.64	2.99
Glu 12	7.75	4.14	2.31, 2.26	2.70, 2.58		
Leu 13	8.07	4.26	1.86, 1.92	1.60, 1.69	0.93, 0.89	
Leu 14	8.06	4.26	1.92, 1.86	1.69, 1.60	0.93, 0.89	
Lys 15	7.77	4.27	1.98	1.58, 1.55	1.77	3.08
Gly 16	8.09	4.01				

as well as six of the thirteen possible $d_{\alpha N}(i,i+3)$ NOEs. The remaining $d_{NN}(i,i+1)$ and $d_{\alpha N}(i,i+3)$ NOEs were unobserved because of spectral overlap. All of the possible $d_{\alpha\beta}(i,i+3)$ NOEs were obscured by spectral overlap. The observation of the majority of the $d_{NN}(i,i+1)$ NOEs gives a strong indication of helicity for most of the peptide. The overlapping set of $d_{\alpha N}(i,i+3)$ NOEs which arise from interactions across a turn of the helix suggests that the helix extends from position 2 to position 15 in the helix. There is a small $d_{NN}(i,i+1)$ NOE from Gly 1 to Glu 2, suggesting that Gly 1 may adopt a helical conformation part of the time.

The $^3J_{\alpha N}$ coupling constants are also presented in Figure 8. The dihedral angle between the amide and α protons is reflected in the coupling constants and can therefore be used to distinguish regular α-helical or β-sheet structures. Coupling constants less than about 6 Hz are typically equated with helical structures in proteins.[31-33] Because most of the amide protons were resolved in the one-dimensional spectrum, $^3J_{\alpha N}$ vicinal coupling constants for α_{1B} could be measured drectly (Figure 8). The coupling constants for the central 14 residues tend to be well below the upper limit of 6 Hz.

Concentration Dependence of the NMR Spectrum of α_1B. An important finding of this work is that there is only one set of resonances associated with α_1B in the tetrameric state. One possible explanation for this observation is that the tetramer might be composed of symmetrically arranged monomers as in the design. Alternatively, the tetramer might be assymetric, but the monomers within the tetramer might appear equivalent on the NMR time scale because of rapid internal motions of the side chains, or rapid association and dissociation of monomers or dimers. The kinetics of the overall association and dissociation of the monomers could be assessed by measuring the spectra under conditions where both the tetramer and the monomer were significantly populated, which was accomplished at pH 3.0 with peptide concentrations ranging from 0.03 to 3.4 mM, corresponding to monomer concentrations ranging from approximately 8% to greater than 99% of the total, respectively (Figure 9). Sharp peaks are observed at high concentrations where the peptide is almost exclusively tetrameric. As the concentration of monomers approaches 50%, a number of the resonances are broadened considerably while others remain sharp. Interestingly, the peaks that remain sharp show very small changes in chemical shift. Some of these peaks include the C-terminal carboxamides and the amides of Gly 1 and Glu 2. This finding indicates that these residues have a similar environment in the monomers and tetramers, suggesting that they may be disordered in the tetramer.

It is unlikely that the broadening of the other resonances is due to exchange of the amide protons with solvent because (i) the rate of proton exchange with solvent would not be sufficient at pH 3.0 to cause such broadening,[30] (ii) the C-terminal carboxamide protons (the most upfield protons), which should be most labile toward exchange with solvent, remain sharp at all concentrations, and (iii) at very low concentrations where the peptide is predominantly monomeric (bottom panel) the peaks become sharp again.

A possible explanation for the broadening is that one of the steps in the monomer to tetramer equilibrium is in intermediate exchange. If the rate of tetramer dissociation is responsible for the intermediate exchange, then the large changes in chemical shift, which appear to be on the order of 300–600 Hz, are indicative of a rate constant for dissociation on the order of 10^2–10^3

(31) Wüthrich, K. *NMR of Proteins and Nucleic Acids*; John Wiley & Sons: New York, 1986.
(32) Karplus, M. *J. Phys. Chem.* **1959**, *30*, 11-15.
(33) Pardi, A.; Billeter, M.; Wüthrich, K. *J. Mol. Biol.* **1984**, *180*, 741-751.

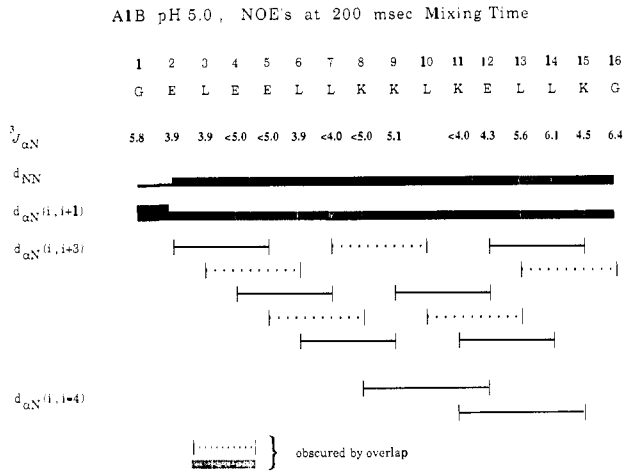

Figure 8. Summary of short and medium range NOEs of α_1B (pH 5.0, 22 °C) from NOESY experiments recorded at 600 MHz and $J_{\alpha N}$ coupling constants (pH 3.0, 45 °C). Sequential $d_{\alpha N}$, d_{NN} NOE connectivities and $d_{\alpha N}(i,i+3)$ connectivities are indicated by bars. Values of $J_{\alpha N}$ are approximate for Glu 4, Glu 5, Leu 7, Leu 8, and Leu 11, as individual lines in the doublet were not resolved. In these cases, upper limits of $J_{\alpha N}$ were based on the widths of the composite peak measured at half-height. The width of the amide resonance of Leu 10 was disproportionally broad, and a reliable value of $J_{\alpha N}$ could not be determined. The assignments of Leu 13 and Leu 14 may be reversed, as these peaks were not resolved in the two-dimensional spectrum.

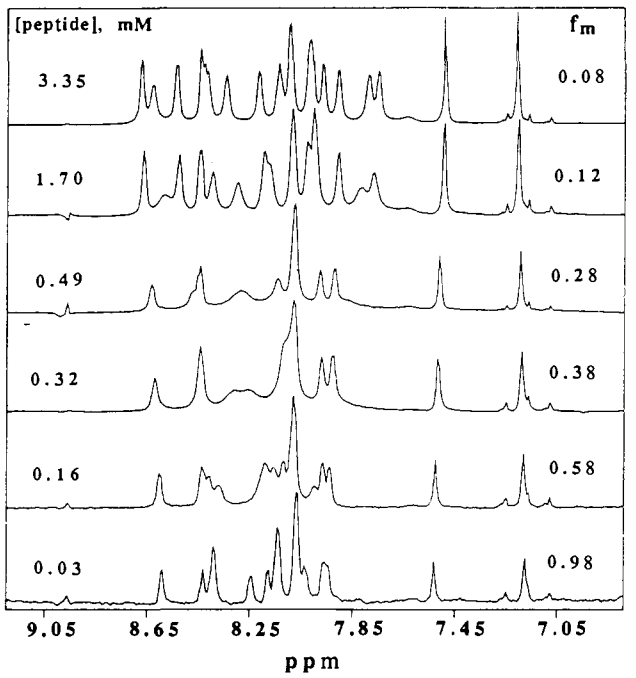

Figure 9. Downfield region of the proton NMR spectrum of α_1B at pH 3.0 as a function of peptide concentration. Peptide concentrations and the corresponding fraction of monomer present, f_m, are shown in the figure. f_m was calculated from the monomer–tetramer association constant.

s^{-1}. If this is the rate-limiting process for monomer formation, then the overall rate of the tetramer to monomer equilibrium must be in this same range at high concentrations where the two-dimensional NMR spectra were recorded. Thus, it is unlikely that the simplicity of the NMR spectra arise from a rapid dissociation and reassociation of tetramers down to individual monomers. Further, at pH 5, the α_1B tetramer is considerably more stable than at pH 3 (Table II), and the dissociation of tetramers might be even slower.

On the other hand, it is possible that a rapid tetramer to dimer equilibrium could account for the simplicity of the spectrum. For example, melittin, an amphiphilic α-helical peptide, forms tetramers according to Scheme II,[34]

$$4M \underset{k_{-1}}{\overset{k_1}{\rightleftharpoons}} 2D \underset{k_{-2}}{\overset{k_2}{\rightleftharpoons}} T$$

where M, D, and T refer to the monomers, dimers, and tetramers of α_1B, respectively. For this peptide, k_1 and k_{-1} limit the rates of association and dissociation, respectively, and the dimer/tetramer equilibrium is relatively rapid. Thus, the NMR spectrum of tetrameric melittin shows a single set of resonances,[35] even though the assymetric unit in the crystal structure is a dimer[36] and the monomers are in slow exchange with the tetramers.[37]

The finding of intermediate exchange for α_1B contrasts with the behavior of the 12-residue peptide, α_1, which shows sharp amide resonances throughout the transition from concentrations where the self-associated form dominates to those where the monomer is the major species.[15] This behavior is likely to be a consequence of the considerably less favorable association constant of α_1 as compared to α_1B at pH 3.

Conclusions

This paper describes the first detailed study of the structural and dynamic properties of α_1B. Using sedimentation equilibrium centrifugation we have confirmed that the protein forms tetramers at pH 7.0 in preference to other aggregation states. The concentration dependence of θ_{222} also suggests that the peptide forms tetramers at pH 5.0 and 3.0, although the stability of the tetramer was considerably decreased at pH 3.0.

The NMR and CD methods used in this work are in good agreement concerning the secondary structure of α_1B. The NMR data indicate that the helical portion of the peptide begins at residue 2 and extends through residue 15, with the terminal Gly residues showing evidence for less complete participation in the helix. This conclusion is in substantial agreement with the CD data, which indicates that 13 of the amides are in an α-helical conformation. The CD data indicate the presence of 3_{10} or turn conformations. A short region of 3_{10} helical conformation at the C-terminal end of the α-helix is frequently observed in globular proteins[29] and would also be consistent with the NMR data.

At present, less can be concluded concerning the overall arrangement of the helices in the tetramer. The observation of only 16 amide resonances tends to support the symmetry incorporated in the design, and we have shown that the simplicity of the spectrum is not a simple consequence of complete dissociation of the peptides to monomers and then reassociation to tetramers. However, the possibility of conformational averaging based on rapid side chain fluctuations or rapidly equilibrating intermediates (e.g., dimers) cannot yet be ruled out. Interhelical NOEs, which would help define the positions of the helices, could not unequivocally be identified due to substantial overlap of the side chain resonances. Even a homonuclear three-dimensional experiment (TOCSY-NOESY) was not helpful in identifying useful NOEs. Current studies using isotopic labeling and amino acid substitutions have the potential of reducing the degeneracy of the side chains.

Acknowledgment. We thank Dr. David Weaver and Dr. Alan Stern for many helpful discussions. We acknowledge support from NSF Grant DMB 8604304 to David Live, NIH and NSF for the purchase of the GN-600 spectrometer at Emory University, and NIH Grant GM-21479 to W. C. Johnson.

(34) Schwarz, G.; Beschiaschvili, G. *Biochemistry* **1988**, *27*, 826–7831.
(35) Brown, L. R.; Lauterwien, J.; Wütrich, K. *Biochim. Biophys. Acta* **1980**, *622*, 23'–244.
(36) Terwilliger, T. C.; Eisenberg, D. *J. Biol. Chem.* **1982**, *257*, 6010–6015.
(37) Weaver, A. J.; Kemple, M. D.; Prendergast, F. G. *Biochemistry* **1989**, *28*, 8614–8623.
(38) Redfield, A. G.; Kuntz, S. D. *J. Magn. Reson.* **1975**, *19*, 250–254.